Damage Development During Pin Loading Of A Hole In A Quasi-Isotropic Carbon Fibre Reinforced Epoxy Composite*

R. Ujjin[1], A. Crosky[2], L. Schmidt[2], D. Kelly[1], R. Li[1] and D. Carr[3]

[1]School of Mechanical Engineering, University of New South Wales, NSW 2052

[2]School of Materials Science and Engineering, University of New South Wales, NSW 2052

[3]Australian Nuclear Science and Technology Organisation, Private Mail Bag 1, Menai, NSW 2234

ABSTRACT: Damage development and progression was monitored by acoustic emission during pin loading of a hole in a quasi-isotropic Hexcel F593/T300 W2G 190 carbon fibre reinforced epoxy composite. Analysis of the acoustic emissions showed that failure was initiated by fibre matrix debonding, followed by fibre fracture, and subsequent matrix cracking. Sections taken through the specimens at varying intervals between the initial acoustic emission and final catastrophic failure confirmed this sequence of events. Good agreement was obtained between the load at the onset of failure and that predicted by finite element modelling.

1 INTRODUCTION

This work was undertaken to establish the onset of damage during bearing loading to evaluate the predictions of a numerical analysis. In previous work, the authors carried out post-mortem microstructural examination of carbon fibre/epoxy composite specimens loaded to varying levels of the ultimate bearing failure load [Ujjin et al., 2003]. This revealed that the principal failure modes were fibre kinking, fibre fracture, fibre-matrix shearing, and matrix cracking, but it was difficult to establish the precise load for failure initiation.

Acoustic emission (AE) provides a nondestructive investigative technique for monitoring damage development in real-time during an actual test. It has been used in previous composite testing programs to monitor damage such as creep damage [Toshiyuki, 1997], delamination [Park, 2001], and damage development during tensile and compressive testing [Ireman et al., 2000, Ageorges et al., 1999]. Moreover, different types of microfailure have been found to give different acoustic signatures and these can be used to identify the different types of damage as they occur.

In the present study, acoustic emission monitoring, coupled with post-mortem microstructural analysis, was employed to evaluate the micro-failure modes of quasi-isotropic and near quasi-isotropic laminates carbon fibre/epoxy laminates. The objectives of this work were to determine the point of failure initiation and the occurrence of subsequent individual micro-cracking events. It was also hoped that an identification of the types of damage that occurred in the laminate would be made possible. In order to discriminate between the different AE waveforms and their corresponding failure modes, it was necessary that differences in amplitude and energy, along with the load-deflection response of the loading pin, were measured and recorded throughout the duration of the test.

Microbuckling theory, in conjunction with the finite element analysis program MSC.MARC, was used to predict failure. This procedure has been used previously to successfully predict bearing failure initiation in non-woven 0º/90º composite laminates [Wu and Sun, 1998]. It focuses on the normal stress (σ_{xx}) and out-of-plane shear stress (τ_{xz}) in pin-loaded laminates. The pin-loaded analysis was used, since it represents the worst case service condition where the original clamping produced by a close tolerance bolt in a fastened joint is lost during service.

*This research was undertaken as part of the research program of the Cooperative Research Centre for Advanced Composite Structures Ltd.

2 EXPERIMENTAL

2.1 Specimens preparation and test procedure

A series of quasi-isotropic carbon fibre/epoxy laminate panels were tested. The panels were made from Hexcel Composites W2G190 prepreg, a bi-directional woven carbon fibre fabric prepreg, impregnated with F593 epoxy resin. Laminates of three different thicknesses, constructed from 24, 16 and 5 plies of prepreg, each ply being 0.21-0.24 mm thick, were examined with two different hole diameters of 10 mm and 20 mm being used. Equal amounts of 0º/90º and ±45º plies were used in the lay up of the panels except in the case of the 5 ply specimens. All specimens were cured in an autoclave at 180°C using the cure cycle recommended by the prepreg manufacturer. Specimens were fabricated with the stacking sequences shown in Table 1.

Table 1. Laminate configurations

Laminate	Stacking sequence
24 Ply	$[\pm45^o\ 0^o/90^o\ \pm45^o\ 0^o/90^o\ 0^o/90^o\ \pm45^o\ 0^o/90^o\ \pm45^o\ \pm45^o\ 0^o/90^o\ \pm45^o\ 0^o/90^o]_s$
16 Ply	$[\pm45^o\ 0^o/90^o\ \pm45^o\ 0^o/90^o\ 0^o/90^o\ \pm45^o\ 0^o/90^o\ \pm45^o]_s$
5 Ply	$[\pm45^o\ 0^o/90^o\ 0^o/90^o\ 0^o/90^o\ \pm45^o]$

Cured specimens were trimmed to approximately 160 mm in length and 70 mm in width. A 20 mm (or 10 mm) hole was drilled 70 mm from the end of each panel along the centerline. The samples were then sectioned across their width through the centre of the hole with the use of a water-cooled circular diamond saw. Following cutting, the bearing area was ground with 600 grit SiC paper to ensure that the surface of the hole was smooth. Grinding was carried out dry, using a cylindrical steel mandrel around which a single layer of SiC paper had been wrapped. The mandrel was mounted in a drill press with the panel in the horizontal plane to ensure that the surface of the hole was ground perpendicular to the surface of the panel. Each sample was checked for smoothness prior to testing using a low power light microscope.

A conventional pin loading setup was used to perform the bearing tests on an Instron 1185 universal testing machine. The lower edge of the specimen was clamped in a steel fixture with adjustable steel support plates to prevent global buckling. The load was applied through 20 mm (or 10 mm) hardened steel pins. The specimens were loaded at a rate of 0.5 mm/min. Figure 1 shows a diagram of the experimental setup with the AE probe and monitor attached.

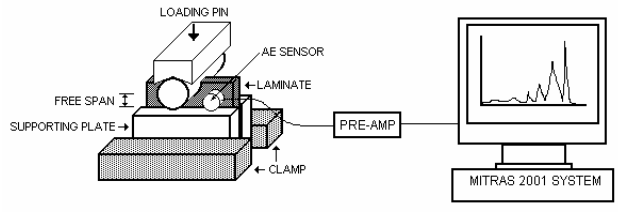

Figure 1. Schematic diagram of AE system and experimental setup

Testing procedure

A set of 6 specimens was first tested to failure to determine the ultimate failure strength and to obtain the approximate load levels at which acoustic emissions occurred. For subsequent tests, the testing was stopped immediately after the 1st, 2nd or 3rd AE signal event. These, together with the panels tested to final failure, provided a set of samples with various levels of damage. Figure 2 shows the pin loading setup on the Instron 1185 testing machine.

Figure 2. Pin loading setup on testing machine

2.2 Acoustic Emission

Acoustic emission has been verified as one of the few successful techniques for detecting failure as it occurs in a laminated composite [Fowler, 1986]. With the application of load onto a composite material there are many mechanisms through which acoustic emissions may be generated. These include resin cracking, fibre fracture, debonding, and interlaminar cracking [Geoff, 1994]. AE techniques can offer real-time information on the characteristics of damage events and fracture of the material [Toshiyuki, 1997]. Analysis of the amplitude distributions provides some guidance; peaks in the spectrum can be associated with specific types of damage events as well as ultimate failure. The AE technique was therefore considered beneficial for the detection of damage initiation generated during this testing program. AE events may also provide information on the nature of damage events that occur during testing.

The system used for failure detection was MISTRAS 2001 AEDSP-32/16 from Physical Acoustics Corporation. This system is a computerised multi-channel system for recording, processing and analysing AE signals. The system consists of a PC with a supplementary data card, the MISTRAS software, AE piezoelectric transducers, and pre-amplifiers. An AE sensor was attached to the specimen using a vacuum grease couplant. The sensor output was amplified at a pre-amplifier. The threshold level was set to 45 dB. The signal was fed into an AE signal processing unit where the AE parameters were analysed using in-built software. The AE signal amplitude and event durations were recorded over the elapsed time. The AE waveforms were then analysed for the characteristic frequencies using a Fast Fourier Transform (FFT). FFT frequency spectra can be used as fingerprints allowing discrimination of the differing failure modes.

3 NUMERICAL ANALYSIS

3.1 Microbuckling failure model

Microbuckling in composites generally results from a geometric instability rather than a material failure due to overstressing [Staab, 1999]. The fibre buckling mechanism can be defined as fibre instability followed by a decreased capability of the fibres to carry load, with the final result being matrix failure through overstressing. There are two distinct modes of fibre buckling in laminar analysis: extension (symmetric) and shear (antisymmetric) modes. The shear mode usually occurs at lower loads and is the relevant mode here. In the shear mode, fibres are assumed to buckle with the same wavelength and are considered to be in phase with each other, as shown in Figure 3(a). In this case, matrix deformation is predominantly in shear [Staab, 1999]. Compressive stress in a fibre due to in-phase buckling leads to the formation of kink zones, with the consequence of deformation of the brittle fibres. Microbuckling of fibres leading to the formation of kink zones with excessive deformation is shown in Figure 3(b). The physical damage [Wu and Sun, 1998] is shown in Figure 3(c)

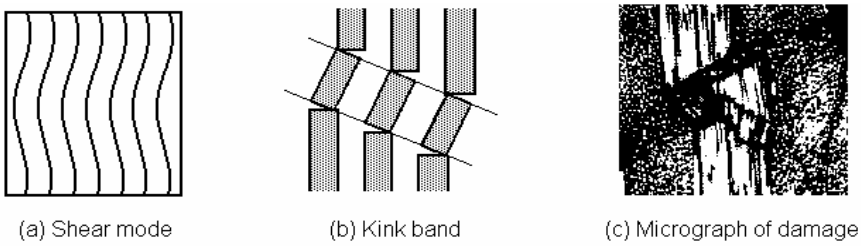

Figure 3. (a) Fibre microbuckling modes in shear (antisymmetric) (b) Schematic of kink band geometry (c) Micrograph of pin-contact damage [Wu and Sun, 1998]

In previous studies [Sun and Jun, 1993, Jun, 1993], an approach from Rosen's energy method [Rosen, 1965] was adopted to derive the elastic fibre microbuckling solution through the use of the Euler-Bernoulli beam-column theory with an elastic foundation. The results for the predicted critical compressive stress for the in-phase (antisymmetric) mode was identical to that reported previously by other workers [Daniel and Ishai, 1994]. The critical compressive stress can be defined as:

$$\sigma_{cr} = \frac{G_m}{1 - c_f} \tag{1}$$

In the present study, a fibre-microbuckling model, previously proposed work [Sun and Jun 1994] was adapted to predict contact failure initiation. As in previous work [Wu and Sun, 1998], the assumption was made that fibre buckling occurs in the through thickness plane. This then permitted evaluation of θ, the ratio of the out-of-plane shear stress, τ_{xz}, to the normal stress, σ_{xx}, from finite element analysis.

$$\theta = \tau_{xz} / \sigma_{xx} \tag{2}$$

3.2 Finite element modelling

The finite element software MSC.MARC was used to perform the 3-D non-linear pin contact analysis. The average normal stress σ_{xx} and out-of-plane shear stress τ_{xz} in the critical volume were both obtained from the model. These were then used to construct the average stress curve for initial failure prediction. The pin-contact model is shown in figure 4.

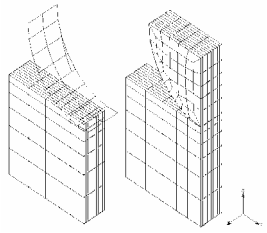

Figure 4. Schematic diagram for 3-D finite element model

4 RESULTS

4.1 Finite element model results

The predicted values of the initial bearing failure load are shown in Table 2. According to the microbuckling theory [Wu and Sun, 1998], bearing failure initiation is most likely to occur at the load level where the load-displacement curve exhibits a second non-linearity. Generally, this is between 70-80 % of the ultimate load. As can be seen from Table 2, good agreement was obtained between the load at the onset of failure and that predicted by non-linear contact analysis in the finite element modeling using the microbuckling criterion, for all three laminates for both pin diameters.

Table 2. Initial bearing failure prediction results

Panel type		24 Ply	24 Ply	16 Ply	16 Ply	5 Ply
Thickness (mm)		5.38	5.38	3.63	3.59	0.88
Pin diameter (mm)		20	10	20	10	20
Peak load (kN)		53.01	27.92	32.82	17.64	7.11
Damage initiation load (kN)	Experiment	42.20	21.26	24.92	13.58	5.41
	FEA	39.37	20.27	23.66	13.02	5.08
% of peak load	Experiment	79.6	76.1	75.9	77.0	76.0
	FEA	74.3	72.6	72.1	73.8	71.4

4.2 Acoustic emission analysis

While the principal aim of the acoustic emission monitoring was to determine the point of damage initiation, it was also found that different failure phenomena occurred during the subsequent course of testing. The first signal consistently appeared with the same waveform and spectrum patterns. For a specific failure mechanism, different AE event spectra were plotted and were again consistently represented by the same pattern. Therefore, it was considered possible to use the frequency spectrum of the AE events as fingerprints characteristic of the physical events from which the AE originated, as reported previously [Ageorges et al., 1999].

During the test the number of hits, duration, amplitude and energy were monitored using the AE system. The failure mechanism determination was then based on the amplitude and width of the AE events within the time domain and frequency spectrum. In the present study, the first signal occurred at an AE amplitude within the 30-50 dB range. The associated characteristic signal appeared in the range of 100-300 kHz. This damage initiation was considered to be fibre matrix debonding [Park et al., 2002]. The second group range was between 50-80 dB. The spectrum associated with this event showed sharp peaks at around 300 kHz. The corresponding failure mode was considered to be fibre breakage [Ageorges et al., 1999]. Once the sample was close to final failure, a wider range of frequencies, in the 0-800 kHz range, was observed and this was considered to be matrix cracking. A combination of the first and second types of waveform occurred simultaneously just before final fracture which was accompanied by a high acoustic emission of around 100 dB. The three distinct AE signals are shown in figure 5.

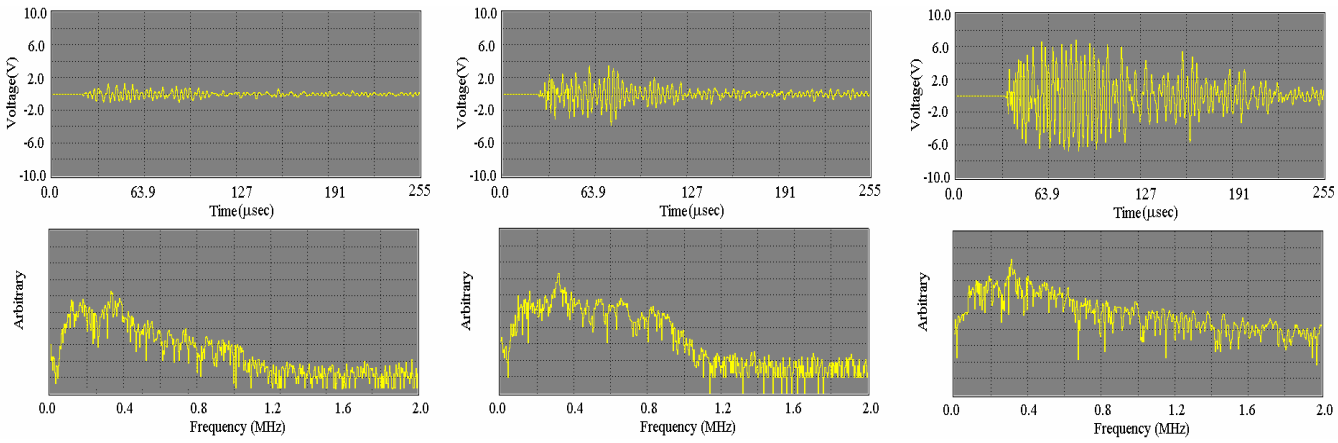

(a) (b) (c)

Figure 5. AE waveforms and their FFT: (a) Interfacial failure, (b) Carbon fibre break and (c) Matrix cracking.

4.3 Microstructural examination

After testing, the specimens were sectioned to determine the internal failure modes associated with each load level and the corresponding AE signal. Following cutting, the sections were polished and examined using a light microscope.

The fracture mechanisms arising from the pin loading contact were correlated with the AE events according to the load level. The corresponding failure modes can be seen in Figure 6. Figure 6(a) shows fibre breakage at a load level between 70-80% of ultimate load. Figure 6(b) shows shear bands, matrix cracking and microbuckling as the load was increased from 80-100% of the ultimate load.

(a) (b)

Figure 6. Micrograph of sectioned specimens; (a) Carbon fibre breakage, (b) Matrix cracking.

5 CONCLUSIONS

The present work demonstrates that acoustic emission signals can provide an indication of bearing failure initiation in a quasi-isotropic carbon fibre reinforced epoxy composite. Bearing failure initiation prediction with the use of a microbuckling criterion has been demonstrated. From the predicted results, it was found that the failure predictions for all types of laminates were within 5% of the theoretically expected values.

Acoustic emission (AE) monitoring, combined with Fast Fourier Transform (FFT) frequency analysis, provides an efficient way to detect damage initiation and monitor subsequent microfailure events. In addition, the FFT spectra of the AE events were shown to exhibit characteristic features for specific types of microfailure thus allowing for use as failure mechanism fingerprints.

ACKNOWLEDGEMENTS

R.Ujjin acknowledges the receipt of a PhD scholarship from the Cooperative Research Centre for Advanced Composite Structures Ltd.

REFERENCES

Ageorges C, Friedrich K, and Ye L, “Experiments to relate carbon-fibre surface treatments to composite mechanical properties”, *Composite Science and Technology*, 59, pp.2101-2113 (1999)

Daniel IM and Ishai O, *Engineering mechanics of composite materials*, Oxford, New York, pp. 90-95 (1994)

Ireman T, Ranvik T and Eriksson I, “On damage development in mechanically fastened composite laminates”, *Composite Structures*, 49, pp. 151-171 (2000)

Fowler, TJ, “Experience with Acoustic Emission Monitoring of Chemical Process Industry Vessels”, *in Progress in Acoustic Emission III*, eds. K. Yamaguchi et al, Japan Soc. Non-Destructive Inspection, Tokyo, pp.150-162 (1986)

Geoff E, *Design and Manufacture of Composite Structures*, Woodhead, pp. 299 (1994)

Jun AW, Compressive strength of unidirectional fiber composites with matrix nonlinearity. *PhD Thesis*, Purdue University (1993)

Park HJ, “Bearing failure analysis of mechanically fastened joints in composite laminates”, *Composite Structure*, 53, pp.199-211 (2001)

Park JM, Kim, JW and Yoon DJ, “Interfacial evaluation and microfailure mechanisms of single carbon fiber/ bismaleimide (BMI) composites by tensile and compressive fragmentation tests and acoustic emission”, *Composite Science and Technology*, 62, pp.743-756 (2002)

Rosen BW, Mechanics of composite strengthening, *Fiber Composite Materials*, *ASMS* (1965).

Staab GH, *Laminar composites*, Butterworth-Heinemann, MA, pp. 166-173 (1999)

Sun CT, Jun AW, “Compressive strength of unidirectional fiber composites with matrix non-linearity”, *Composite Science and Technology*, 52, pp. 577-587 (1994)

Sun CT, Jun AW (1993) Effect of matrix nonlinear-behavior on the composite strength of fiber composites. *Mechanics of Thick Composites*, 162, pp. 91-105 (1994)

Toshiyuki, “Acoustic emission monitoring of the progress of damage during a short-term creep test on notched plain woven e-glass/epoxy composites”, *Advances in Fiber Composite Materials*, Elsevier Science, pp. 81 (1997)

Ujjin R, Li R, Kelly DW and Crosky A, “Prediction of bearing failure in pin loaded fibre laminates”, *AIAC* (2003)

Wu PS, Sun CT, “Bearing failure in pin contact of composite laminates”, *AIAA Journal*, 36(11), pp. 2124-2129 (1998)

Wu PS, Sun CT, “Modeling bearing failure initiation in pin-contact of composite laminates”, *Mechanics of Materials*, 29, pp. 325-335 (1998)